New Substrates for the Oscillating Briggs−Rauscher Reaction

Stanley D. Furrow,*,† Rinaldo Cervellati,‡ and Giovanna Amadori‡

Department of Chemistry, Berks-Lehigh Valley College, Pennsylvania State University, Reading, Pennsylvania 19610-6009, and Dipartimento di Chimica G. Ciamician, Università di Bologna, via Selmi 2, 40126 Bologna

Received: October 18, 2001; In Final Form: April 19, 2002

Several new organic substrates have been found to promote oscillations in batch conditions in the Briggs−Rauscher oscillating system. The new substrates, crotonic acid, acrylic acid, anisole, and *p*-nitrophenol, react with iodine (I) by either addition or substitution reactions. Rate constants for reactions of these four compounds with HOI have been determined. Previously known substrates have active methylene hydrogens and react with I_2 via an enol mechanism. Some type of active reduction of HIO_2 to HOI (other than by iodide) must be included in the mechanism to allow the simulation of oscillations with the new substrates.

1. Introduction

As stated by Furrow and Noyes,[1] the most dramatic oscillating reaction in solution is probably that discovered by Briggs and Rauscher,[2] referred to here as the BR reaction. When appropriate amounts of hydrogen peroxide, acidic iodate, manganous salt, malonic acid (MA), and starch indicator are mixed in aqueous solution, the system repeats a yellow → blue → colorless sequence several times. The BR systems described to date have used acetone or MA and its derivatives as organic substrates.[3]

During the oscillatory regime, there is a periodic consumption and production of I_2, iodide ion, and other intermediates. Furrow[4] found that the addition of crotonic acid (CA) to the iodine production (IP) subsystem, H_2O_2, IO_3^-, H^+, and Mn(II), leads to a change in the rate equation for iodate reduction. In fact, CA reacts quickly with HOI, a precursor of I_2 in the IP subsystem, to form a stable iodohydrin.[5] Phenol is a still more effective scavenger of iodine in low oxidation states.[6] Phenol in concentrations of 10^{-4} M prevents I_2 production in the IP subsystem and completely inhibits oscillations when added to an active MA oscillator. CA and certain phenolic substances can, however, act as substrates for the BR system instead of acetone or MA.

MA and its derivatives consume I_2 via the enol form to give an iodoproduct and iodide ion, whereas CA and phenol are iodinated by HOI, and there is indirect formation of iodide from I_2 hydrolysis.

We present here in detail the behavior of CA, acrylic acid (AC), anisole (AN), and 4-nitrophenol (pNP) oscillators.[7] We present a modified pathway to account for oscillations with the new substrates.

2. Experimental

Double-distilled water was used to prepare all solutions. Reagent grade chemicals were used when available. Crotonic acid was recrystallized from water, pNP was recrystallized from toluene, methylmalonic acid was recrystallized from ethyl acetate, and anisole was redistilled. Perchloric acid (70%) was diluted to approximately 1 M or 0.5 M and then analyzed by titration against sodium carbonate. Hydrogen peroxide concentration was determined initially by iodimetric methods. Hydrogen peroxide standards were prepared at several concentrations by dilution; the absorbance at each concentration was read at several wavelengths. Calibration curves were prepared. From then on, $[H_2O_2]$ was calculated from the measured absorbance at several wavelengths and calibration curves.

Iodide concentrations were measured with an Orion model no. 9453 iodide selective electrode versus a double-junction electrode with a silver/silver chloride reference, Orion model no. 90-02. Absorbance measurements were made on a HP 8451A spectrophotometer. All solutions were thermostated at 25.0 ± 0.1 °C. The reaction vessel was a 25-mL three-necked flask. It was immersed to the necks in water in a double-walled beaker through which thermostated water was circulated. Magnetic stirring was applied with a stirring bar and a magnetic stirrer below. Electrodes were sealed to the flask with thin neoprene gaskets. Reagents were admitted by pipet or buret through the third opening, which was later sealed with a Teflon stopper. Some additional details are included later under specific mixtures.

For several kinetic runs, $NaClO_4$ was added to bring the total ionic strength up to 0.200 M. We were not able to discern a trend in salt effects from approximately slightly below 0.1 M up to 0.2 M.

3. Kinetic Study of Subsystems: Substrate, IO_3^-, H^+, I_2

Previously reported oscillatory BR mixtures all have a substrate with an active methylene hydrogen that is replaced by iodine via an enol mechanism. The rate law is of the form $-d[\text{substrate}]/dt = k_a[\text{substrate}][I_2]/\{1 + k_b[I_2]\}$. In solutions containing acidic iodate, methylenic substrates react by

$$5RH + 5I_2 \rightarrow 5RI + 5H^+ + 5I^-$$

coupled with

$$6H^+ + IO_3^- + 5I^- \rightarrow 3I_2 + 3H_2O$$

to give overall

$$H^+ + 5RH + 2I_2 + IO_3^- \rightarrow 5RI + 3H_2O$$

* Corresponding author. E-mail: f13@psu.edu. Fax: 610-396-6024.
† Pennsylvania State University.
‡ Università di Bologna.

10.1021/jp0138779 CCC: $22.00
Published on Web 05/29/2002

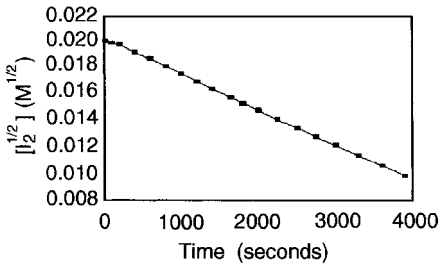

Figure 1. $[I_2]^{1/2}$ vs time for hydroxyiodination of acrylic acid. $[HClO_4] = 0.124$ M, $[KIO_3] = 0.010$ M, [AC] = 0.292 M, and $[I_2]_0 = 4.1 \times 10^{-4}$ M.

None of the new substrates contains active methylene hydrogens, but they all have a region of unsaturation. With aromatic substrates, the overall stoichiometry is the same as above,

$$H^+ + 5ArH + 2I_2 + IO_3^- \rightarrow 5ArI + 3H_2O$$

because substitution occurs on the ring.

With aliphatic unsaturated substrates, addition takes place, forming the iodohydrin:

$$H^+ + 5R + 2I_2 + IO_3^- + 2H_2O \rightarrow 5RHOI$$

The mechanisms are different for each of these iodinations, so we carried out kinetic studies that allowed us to predict the reaction rates.

The kinetics of the subsystem CA, IO_3^-, H^+, and I_2 were previously investigated by Furrow.[5] Similar studies are needed to determine the rate constant of each substrate's iodination so that it can be applied to the complete oscillator.

Spectrophotometry was used to measure the absorbance of I_2 at 460 nm as a function of time, varying one of the initial concentrations each run. Except for anisole (explained below), plots of $[I_2]^{1/2}$ versus time are nearly straight, indicating psuedohalf order in $[I_2]$. (The concentrations of all the other species are much higher than $[I_2]$). A sample plot is shown in Figure 1. Because the rate expression is well-represented by

$$-d[I_2]/dt = k'[I_2]^{1/2}$$

from the integrated form, the slope of $[I_2]^{1/2}$ versus t is equal to $-2k'$, and

$$k' = k_{app}[H^+]^a[substrate]^b[IO_3^-]^c$$

The orders in $[H^+]$, [substrate], and $[IO_3^-]$ were found from plots of ln(−slope) versus ln(concentration). An example is shown in Figure 2. After the order was found for each reactant, the apparent rate constant, k_{app}, was evaluated from the slope of each run. Table 1 shows the results from acrylic acid runs.

The rate equations obtained for all substrates were close to

$$-d[I_2]/dt = k_{app}[H^+]^1[substrate]^{1/2}[IO_3^-]^{1/2}[I_2]^{1/2} \quad (I)$$

although there were significant deviations in the orders of $[H^+]$ and $[IO_3^-]$ as noted below.

A set of steps is suggested in Table 2. The steps are similar to a mechanism previously proposed for CA.[5]

Step 1 is a relatively fast equilibrium. Step 2 is fast and is coupled with step 3, the Dushman reaction. Reaction 4 involves electrophilic attack on the double bond or on the aromatic ring in the substrate by H_2OI^+ or possibly I^+. We have not added

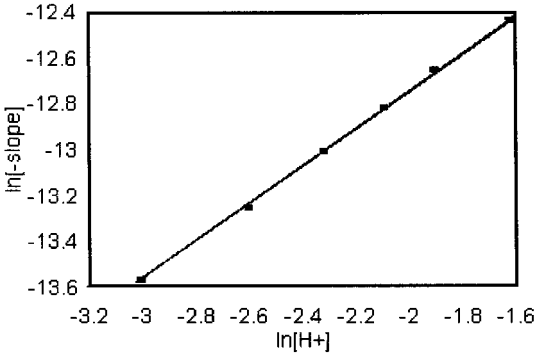

Figure 2. ln(−slope) vs $ln[H^+]$ for the hydroxyiodination of acrylic acid. $[KIO_3] = 0.010$ M, [AC] = 0.292 M, and $[I_2]_0 = 4.1 \times 10^{-4}$ M.

TABLE 1: Summary for Hydroxyiodination of Acrylic Acid[a]

$[HClO_4]_0$ (M)	$[KIO_3]_0$ (M)	$[NaClO_4]_0$ (M)	$[AC]_0$ (M)	−slope[b] ($M^{1/2}/s$) × 10^6	$[I_2]_0$ (M) × 10^4	k_{app}[c]
0.0496	0.0100	0.1	0.292	1.28	4.22	0.000578
0.074	0.0100	0.075	0.292	1.78	4.16	0.000576
0.074	0.0100	0	0.292	1.75	4.11	0.000566
0.091	0.0091	0	0.0859	1.04	5.43	0.000552
0.0991	0.0100	0	0.292	2.23	4.12	0.000566
0.100	0.0100	0	0.219	1.96	5.87	0.000572
0.124	0.0100	0	0.292	2.69	4.09	0.000567
0.125	0.0067	0	0.0558	0.95	4.35	0.000561
0.149	0.0100	0	0.292	3.20	4.08	0.000579
0.198	0.0100	0	0.292	3.97	3.99	0.000568

[a] Concentrations were corrected for extent of reaction. [b] −Slope of $[I_2]^{1/2}$ versus time. [c] Rate constants at 25 °C in the equation $-d[I_2]/dt = k_{app}[H^+]^{0.83}[AC]^{1/2}[IO_3^-]^{1/2}[I_2]^{1/2}$.

TABLE 2: General Reaction Sequence for Iodination or Hydroxyiodination

reaction/rate law	
$I_2 + H_2O \rightleftharpoons HOI + I^- + H^+$ $-d[I_2]/dt = k_1[I_2]/[H^+] - k_{1R}[HOI][I^-]$	(1), (1R)
$HIO_2 + I^- + H^+ \rightarrow 2HOI$ $-d[HIO_2]/dt = k_2[HIO_2][I^-]$	(2)
$IO_3^- + I^- + 2H^+ \rightarrow HOIO + HOI$ $-d[IO_3^-]/dt = k_3[H^+]^2[IO_3^-][I^-]$	(3)
$H^+ + HOI + substrate \rightarrow H^+ + iodoproduct\ (+ H_2O)$ $-d[substrate]/dt = k_4[H^+][HOI][substrate]$	(4)

the fast equilibria with HOI and H^+ nor those with IO_3^-, H^+, and HIO_3, so we are using [HOI] and $[IO_3^-]$ to represent total [I(I)] and [I(V)], respectively.

The rate expression derived from the above mechanism by assuming steady-state [HOI], $[I^-]$, and $[HIO_2]$ is

$$-d[I_2]/dt = -^2/_5\, d[substrate]/dt = {}^2/_5(5K_1k_3k_4)^{1/2}[H^+][substrate]^{1/2}[IO_3^-]^{1/2}[I_2]^{1/2} \quad (II)$$

The rate constants for steps 1, 2, and 3 are known, so k_4 can be evaluated. Recently, Agreda, Field, and Lyons[8] (AFL) restudied the Dushman reaction kinetics (step 3) and concluded that the rate law has a second-order term in $[I^-]$, although their study did not extend to the low $[I^-]$ encountered in this work. The steady-state $[I^-]$ in our experiments is below 10^{-6}M, as it is in the region where second-order iodide kinetics would be expected from the AFL model. If the AFL model is used for the Dushman reaction, then the exponent on $[IO_3^-]$ and [substrate] in the derived rate law would be $^1/_3$ for each and $^2/_3$ on $[I_2]$. These values are significantly different from the experimental values from our data. For that reason, we have a used first-order iodide dependence in the Dushman reaction.

TABLE 3: Additional Reaction Steps for Hydroxyiodination of Acrylic Acid

reaction/rate law	
$H^+ + HOI + AC \rightarrow H^+ + HOIAC$ $-d[AC]/dt = k_4[H^+][HOI][AC]$	(4)
$HOI + AC \rightarrow HOIAC$ $-d[AC]/dt = k_5[HOI][AC]$	(5)

TABLE 4: Average Rate Constants for the Reaction of I(I) with Acrylic Acid

step	value	comments
(4)	$k_4 = 807 \pm 46\ M^{-2}\ s^{-1}$	from slope of k_4' $[H^+]$ vs $[H^+]$
(5)	$k_5 = 35 \pm 6\ M^{-1}\ s^{-1}$	from intercept of k_4' $[H^+]$ vs $[H^+]$

Because the order in iodate is significantly more than $^1/_2$ for CA and AN reactions and the order in $[H^+]$ is different from 1 with AC, pNP, and AN reactions (see below), there must be contributions from steps that are not included in the mechanism reported in Table 2. For simulation purposes, we have assumed that most of the substrate reaction in our solutions is accounted for by the mechanism above and have modified the mechanism to take account of the differences in order from that predicted by I. The modifications are outlined below under each substrate.

3.1. Subsystem: Acrylic Acid, IO_3^-, H^+, I_2. The acrylic acid subsystem deviates from rate law I with a lower dependence on $[H^+]$, with order 0.83 instead of 1.0.

$$-d[I_2]/dt = k_{app}[H^+]^{0.83}[AC]^{1/2}[IO_3^-]^{1/2}[I_2]^{1/2} \qquad \text{(III)}$$

Plots of $[I_2]^{0.5}$ versus t are straight for at least 80% of the loss of I_2. For unknown reasons, the data points in this subsystem taken sooner than 100 s were often slightly below the straight line and have been omitted from the determination of the slope. (The duration of the runs was from 2800 to 8000 s).

Because steps 1−3 are common to all the substrates, we look to some variation in step 4. The simplest postulate was to assume an attack of neutral HOI on the acrylic acid, as well as step 4. See Table 3.

Setting steady-state values as we did above, the result is

$$-d[I_2]/dt = -^2/_5\, d[AC]/dt = {}^2/_5(5K_1k_3)^{1/2}(k_5 + k_4[H^+])^{1/2}[H^+]^{1/2}[AC]^{1/2}[IO_3^-]^{1/2}[I_2]^{1/2} \qquad \text{(IV)}$$

Comparison of this relation with eq III gives

$$k_{app}\,[H^+]^{0.83} = ({}^2/_5)(5K_1k_3)^{1/2}(k_5 + k_4[H^+])^{1/2}[H^+]^{1/2}$$

which can be rearranged to

$$({}^5/_4)(k_{app})^2[H^+]^{0.66}/(K_1k_3) = k_5 + k_4[H^+]$$

Plotting the left side versus $[H^+]$ for all the runs gives $k_4 = 719 \pm 31\ M^{-2}/s$ and $k_5 = 44 \pm 4\ M^{-1}/s$.

This method relies on approximations about changes in [AC], $[H^+]$, and $[IO_3^-]$ during the reaction and equilibrium being maintained in the iodine hydrolysis reaction. This situation is not strictly true and leads to a small error in k_4. A superior method, we believe, is numerical integration. We used the Gepasi simulator[9] in the fitting mode with the above mechanism to find the best fit for k_4 for each run with k_5 set to 0. We use the symbol k_4N for that specific k_4. Then, setting k_5 to 0 in IV, one can equate $k_4N[H^+]$ to $k_5 + k_4[H^+]$. Plotting $k_4N[H^+]$ versus $[H^+]$ for all the runs gives values of k_4 and k_5 from the slope and intercept. See Table 4.

3.2. Subsystem: Crotonic Acid, IO_3^-, H^+, I_2. Crotonic acid runs have straight-line plots of $[I_2]^{0.5}$ versus t, but runs with differing initial $[IO_3^-]$ showed that the order in $[IO_3^-]$ was 0.65 instead of 0.50. Only a few runs were carried out to confirm the previous study.[5] See Table 5.

For crotonic acid, the rate law is

$$-d[I_2]/dt = k_{app}[H^+]^1[CA]^{1/2}[IO_3^-]^{0.65}[I_2]^{1/2} \qquad \text{(V)}$$

To account for the order in $[IO_3^-]$ being greater than $^1/_2$, it appears that after electrophilic attack by H_2OI^+ or I^+ on the double bond there could be two parallel paths to a product, one in which IO_3^- is involved either in bringing −OH to the adjacent carbon or in breaking the I−O bond in H_2OI^+. Therefore, we have added the steps shown in Table 6.

We do not have enough information to determine k_{4R} separately, so we assumed an arbitrary value. We then set a ratio of k_6 to k_7 such that the order of 0.65 in iodate would follow. We essentially followed a trial and error process with Gepasi to find k_6 and k_7 with the proper ratio such that all the runs over the range of $[IO_3^-]$ that were tested gave k_4 with no trends. The value of k_{4R} was adjusted to give a low standard deviation between measured and simulated $[I_2]$ values. See Table 7.

3.3. Subsystem: *p*-Nitrophenol, IO_3^-, H^+, I_2. We used a method similar to that used for CA to find that the rate law for the iodination of *p*-nitrophenol is as follows:

$$-d[I_2]/dt = k_{app}[H^+]^{0.92}[pNP]^{1/2}[IO_3^-]^{0.62}[I_2]^{1/2} \qquad \text{(VI)}$$

See Table 8.

We set the iodate dependence using runs with varying initial $[IO_3^-]$ and set $[H^+]$ dependence using runs with varying initial $[H^+]$.

There is evidence that the final product of iodination of pNP is 2,5-diiodo-4-nitrophenol. The diiodo product is rather insoluble and can be separated. The NMR spectrum is consistent with disubstitution. In a run with very low initial [pNP] that lasted more than 72 h, the ratio of I_2 consumed to initial [pNP]

TABLE 5: Summary for Hydroxyiodination of Crotonic Acid

$[HClO_4]_0$ (M)	$[KIO_3]_0$ (M)	$[NaClO_4]_0$ (M)	$[CA]_0$ (M)	−slope[a] $[M]^{1/2}\ s^{-1} \times 10^6$	$[I_2]_0$ (M) $\times 10^4$	k_{app}[b] $(M^{-1.65}\ s^{-1})$	$k_4 \times 10^{-4}$ [c] $(M^{-2}\ s^{-1})$
0.125	0.0067	0.0000	0.0225	1.38	4.02	0.00396	5.25
0.125	0.0050	0.0700	0.100	2.40	4.07	0.00387	5.63
0.125	0.0100	0.0650	0.100	3.69	4.05	0.00377	5.80
0.125	0.0200	0.0550	0.100	5.67	4.03	0.00367	5.70
0.125	0.0400	0.0350	0.100	9.12	3.99	0.00376	5.62
0.125	0.0750	0.0000	0.100	14.0	3.57	0.00383	5.76

[a] −Slope of $[I_2]^{1/2}$ versus time. [b] Rate constants at 25 °C in the equation $-d[I_2]/dt = k_{app}\,[H^+]^1\,[CA]^{1/2}\,[IO_3^-]^{0.65}\,[I_2]^{1/2}$. Initial concentrations were corrected for the extent of reaction. [c] Rate constants at 25 °C in the equation $-d[CA]/dt = k_4\,[H^+][HOI][CA]$ from numerical integration. See text.

TABLE 6: Additional Reaction Steps for Hydroxyiodination of Crotonic Acid

reaction/rate law	
$H^+ + HOI + CA \rightleftharpoons H_2OICA^+$ $-d[CA]/dt = k_4[H^+][HOI][CA] - k_{4R}[H_2OICA^+]$	(4), (4R)
$H_2OICA^+ \rightarrow HOICA + H^+$ $-d[H_2OICA^+]/dt = k_6[H_2OICA^+]$	(6)
$H_2OICA^+ + IO_3^- \rightarrow HOICA + IO_3^- + H^+$ $-d[H_2OICA^+]/dt = k_7[H_2OICA^+][IO_3^-]$	(7)

TABLE 7: Average Rate Constants for the Reaction of I(I) with Crotonic Acid

step	value	comments
(4)	$k_4 = (5.63 \pm 0.19) \times 10^4\ M^{-2}\ s^{-1}$	average of least-squares fits
(4R)	$k_{4R} = 0.10\ s^{-1}$	arbitrary
(6)	$k_6 = 0.0084\ s^{-1}$	to fit $[IO_3^-]$ data
(7)	$k_7 = 0.34\ M^{-1}\ s^{-1}$	to fit $[IO_3^-]$ data

was approximately 4:5, which is also consistent with diiodo substitution. The second iodination is believed to be slower than the first, but not negligible. We simultaneously found the best fit for both the first (k_4) and second iodinations (k_8) in a long-lasting run with initially low [pNP] and high $[I_2]$. We then used that value as the fixed second iodination constant and allowed the Gepasi program to fit the first constant for all the remaining runs. See Table 9.

An iterative process was used to set k_9 so that the simulation would match the order in $[H^+]$ on the basis of protonation of pNP, which should inhibit electrophilic attack. The values for k_4, k_6, k_7, and k_{4R} were set using a process similar to that used with CA above, assuming an equilibrium addition, followed by either an uncatalyzed or iodate-catalyzed path to product. See Table 10.

3.4. Subsystem: Anisole, IO_3^-, H^+, I_2. Determination of the rate law is complicated because of slight but noticeable curvature in plots of $[I_2]^{1/2}$ versus t, indicating an order in $[I_2]$ somewhat greater than $^1/_2$. Therefore, orders were determined by using the initial rate method; initial slopes of $[I_2]$ versus t were calculated from least-squares fits of quadratic curves. Orders were calculated from slopes of ln[−slope] versus ln[concentration]. See Table 11.

For anisole, the rate law is

$$-d[I_2]/dt = k_{app}[H^+]^{1.18}[AN]^{1/2}[IO_3^-]^{0.65}[I_2]^{0.55} \quad \text{(VII)}$$

This study has also been complicated by the formation of a precipitate during the recording, limiting the time that the reaction could be followed, and by the strong volatilization of the anisole itself. To minimize the latter problem, all the recordings were performed in a gastight flask. Recording was stopped when absorbance near 700 nm began to increase, indicating scattering from precipitate formation.

The precipitate has been carefully studied[10] in two different ways:

(1) We filtered and recrystallized it with a mixture of water and MeOH. From the melting point and the NMR spectrum, we identified it to be 4-I-anisole.

(2) An HPLC study of both the solution and the precipitate dissolved in MeOH confirmed the precipitate to be 4-I-anisole; in the solution, a small amount of 2-I-anisole and traces of 2,4-diiodoanisole were also found.

The inclusion of H^+ in step 4 generates an order of 1 in $[H^+]$. The fact that the order is higher than 1 indicates further involvement of $[H^+]$, but the mechanism is still unknown. We have assumed a reversible attack of protonated HOI (H_2OI^+) on anisole, with two pathways to the iodo product. One of the pathways is uncatalyzed, and the other is catalyzed by H^+ and IO_3^-. With inclusion of the catalyzed pathway, the order in $[IO_3^-]$ is increased above $^1/_2$, and the order in $[H^+]$ is increased above 1.

Iodination of anisole by I_2 is also possible:

$$AN + I_2 \rightarrow ANI + I^- + H^+$$

To the extent that this reaction is important, the order in both $[I_2]$ and [anisole] would be raised above $^1/_2$. These values provide a better fit for I_2 but a poorer fit for anisole compared to experiment. Experiments without iodate present (only I_2, anisole, and acid) indicated very slow reaction by the direct $AN + I_2$ route.

It is conceivable, however, that I_2 and anisole could form an intermediate. If the intermediate was attacked by HOI, an HOI_2^- ion could be formed (which could be protonated and then decompose to I_2 and water), leaving a ANI^+ ion, which could

TABLE 8: Summary for Iodination of *p*-Nitrophenol[a]

$[HClO_4]_0$ (M)	$[KIO_3]_0$ (M)	$[KI]_0$ (M)	$[pNP]_0$ (M)	−slope[b] $(M^{1/2}\ s^{-1}) \times 10^7$	k_{app}[c] $(M^{-1.54}\ s^{-1})$	$k_4 \times 10^{-4}$[d] $(M^{-2}\ s^{-1})$
0.125	0.00500	0.00046	0.0113	5.97	0.00206	2.87
0.125	0.00500	0.00088	0.0113	6.93	0.00243	3.99
0.125	0.0200	0.00083	0.0113	14.8	0.00216	2.81
0.125	0.0100	0.00090	0.0113	8.97	0.00203	2.95
0.125	0.00690	0.00090	0.0113	6.96	0.00199	2.76
0.192	0.00895	0.00083	0.0113	13.0	0.00225	3.52
0.200	0.00690	0.00069	0.0113	11.0	0.00211	3.23
0.050	0.00690	0.00090	0.0113	3.09	0.00208	3.12
0.125	0.00500	0.00090	0.0113	6.25	0.00219	3.24
0.125	0.0100	0.00090	0.0163	11.1	0.00209	3.25
0.125	0.0100	0.00090	0.0045	6.40	0.00229	3.73
0.125	0.00300	0.00090	0.0113	4.30	0.00210	2.73
0.125	0.0100	0.00086	0.00788	8.13	0.00220	3.58
0.125	0.0100	0.00087	0.00563	6.37	0.00204	2.92
0.125	0.0100	0.00087	0.0045	6.02	0.00215	3.28
0.125	0.0100	0.00163	0.0015	3.30	0.00208	2.77

[a] I_2 was formed from the initial fast reaction with KIO_3 and KI. Corrections were made to $[H^+]$, $[IO_3^-]$, and $[I^-]$. Initial concentrations were corrected for the extent of reaction. [b] −Slope of $[I_2]^{1/2}$ versus time, corrected for the extent of reaction in $[H^+]$, $[IO_3^-]$, and [pNP]. [c] Rate constants at 25 °C in the equation $-d[I_2]/dt = k_{app}[H^+]^{0.92}[pNP]^{1/2}\ [IO_3^-]^{0.62}[I_2]^{1/2}$. [d] Rate constants at 25 °C in the equation $-d[pNP]/dt = k_4\ [H^+][HOI][pNP]$ from numerical integration. See text.

TABLE 9: Additional Reaction Steps for Iodination of *p*-Nitrophenol

reaction/rate law	
$H^+ + HOI + pNP \rightleftharpoons H_2OIpNP^+$ $-d[pNP]/dt = k_4[H^+][HOI][pNP] - k_{4R}[H_2OIpNP^+]$	(4), (4R)
$H_2OIpNP^+ \rightarrow IpNP + H^+ + H_2O$ $-d[H_2OIpNP^+]/dt = k_6[H_2OIpNP^+]$	(6)
$H_2OIpNP^+ + IO_3^- \rightarrow IpNP + IO_3^- + H^+ + H_2O$ $-d[H_2OIpNP^+]/dt = k_7[H_2OIpNP^+][IO_3^-]$	(7)
$H^+ + HOI + IpNP \rightarrow I_2pNP^+ + H_2O + H^+$ $-d(IpNP]/dt = k_8[H^+][HOI][IpNP]$	(8)
$pNPH^+ \rightleftharpoons H^+ + pNP$ $d[pNP]/dt = k_9[pNPH^+] - k_{9R}[pNP][H^+]$	(9)

TABLE 10: Average Rate Constants for the Reaction of I(I) with 4-Nitrophenol

step	value	comments
4	$k_4 = (3.2 \pm 0.4) \times 10^4\ M^{-2}\,s^{-1}$	least-squares fit to data
4R	$k_{4R} = 0.8\ s^{-1}$	arbitrary
6	$k_6 = 0.1\ s^{-1}$	to fit $[IO_3^-]$ data
7	$k_7 = 2.88\ M^{-1}\,s^{-1}$	to fit $[IO_3^-]$ data
8	$k_8 = 1700\ M^{-2}\,s^{-1}$	least squares, very long run
9	$k_9 = 4.5 \times 10^9\ s^{-1}$	to fit $[H^+]$ data
9R	$k_{9R} = 1 \times 10^{10}\ M^{-1}\,s^{-1}$	near diffusion control

lose a proton to give iodoanisole. The incorporation of such steps led to an improved fit (of absorbance vs time) for nearly every run. The constants, however, were not consistent from one run to the next; therefore, those steps have not been used here. The means by which the order in $[I_2]$ is slightly higher than $^1/_2$ has not been identified. See Tables 12 and 13.

3.5. Other Subsystems. Searches have been made for other modes of reaction including substrate + iodate, substrate + I(III), and iodosubstrate + iodate or I(III). None of these seems to befast enough to make a significant contribution to the overall reaction rates.

4. Results for Oscillating Systems

4.1. Comparison with Enolic Substrates. Previously reported variations of the Briggs−Rauscher oscillator have used substituted malonic acid or other substances with enol-forming methylene groups. As stated in section 3, the overall stoichiometry is similar for the enolic and unsaturated substrates.

Crotonic acid has been used previously as a sink for I_2 in mixtures with the same components, but oscillations were not observed at that time.[4] After it was established that crotonic acid could serve as a substrate for an oscillator, acrylic acid was tried to check the generality of addition substrates, and then pNP and AN were tried to determine if substitution substrates could also function in a similar way. (It was shown previously that phenol is a powerful inhibitor of oscillations,[6] so pNP was selected as a substance that would react more slowly).

Compared to traditional BR oscillators, the new substrates are more sensitive to operating conditions, and all of the components have more limited ranges of concentration where oscillations occur. The iodide concentration does not rise as high as it does with the methylenic substrates, and the range of the maximum and minimum $[I^-]$ is less. The concentration of I_2 and the range of $[I_2]$ (maximum to minimum) is also less with the new substrates. The new substrate oscillators always end up nearly free of I_2 color. (Iodomalonic acid will often decompose autocatalytically, and malonic acid oscillators can end with solid I_2 precipitating). Thus, the iodo products from the new substrates tend to be more stable than iodomalonic acid in terms of less decomposition. During oscillations with the new substrates, the reacting solutions are mostly in the relatively high iodide region, with narrow spikes into the low iodide region. The period length tends to be somewhat insensitive to concentration variables, so the longer-lived oscillators tend to have the most oscillatory cycles.

Each of the new substrates is discussed separately below.

4.2. Crotonic Acid Oscillators. Each of the components in CA oscillators has a maximum and a minimum in the concentration range where oscillations are observed. The ranges are somewhat interdependent, but roughly, oscillations were found for $[H_2O_2]$ from 0.5 to >1 M, for $[IO_3^-]$ from 0.0033 to > 0.01 M, for $[Mn^{2+}]$ from 0.0023 to >0.033 M, for [CA] from <0.01 to >0.055 M, and for $[HClO_4]$ from ~0.05 to >0.13 M. As a limiting concentration is approached, there is a decrease in both the amplitude and number of oscillations. Typical runs are shown in Figure 3 and Table 1S (Supporting Information).

The first period was usually significantly longer than the following periods. From the second period on, there was a more gradual shortening of the period length. The period length was

TABLE 11: Summary for Iodination of Anisole

$[HClO_4]_0$ (M)	$[KIO_3]_0$ (M)	$[anisole]_0$ (M)	$[I_2]_0$ ($M\,s^{-1}$) × 10^4	$-d[I_2]/dt$ ($M\,s^{-1}$) × 10^8	k_{app}[a] ($M^{-1.85}\,s^{-1}$)	$k_4 \times 10^{-4}$ [b] ($M^{-2}\,s^{-1}$)
0.15	0.0200	0.00215	3.99	6.73	0.00955	5.05
0.075	0.0200	0.00165	4.08	2.59	0.00947	5.17
0.050	0.0200	0.0016	4.06	1.58	0.00953	5.02
0.124	0.0200	0.00816	3.99	10.4	0.00950	5.36
0.124	0.0200	0.00408	4.01	7.31	0.00942	5.15
0.124	0.0200	0.00204	3.95	5.01	0.00920	5.09
0.124	0.0200	0.00102	3.93	3.63	0.00945	5.05
0.199	0.0200	0.0039	3.96	12.6	0.00952	5.35
0.124	0.0200	0.00408	4.01	7.31	0.00942	5.15
0.050	0.0200	0.00387	4.04	2.43	0.00944	4.67
0.124	0.0800	0.00393	4.01	19.0	0.00986	5.16
0.124	0.0200	0.00408	4.01	7.31	0.00942	5.15
0.124	0.0050	0.00393	3.99	2.95	0.00983	5.27

[a] Rate constants at 25 °C in the equation $-d[I_2]/dt = k_{app}\,[H^+]^{1.19}[AN]^{1/2}[IO_3^-]^{0.66}[I_2]^{1/2}$. Initial concentrations were corrected for extent of reaction. [b] Rate constants at 25 °C in the equation $-d[AN]/dt = k_4\,[H^+][HOI][AN]$ from numerical integration. See text.

TABLE 12: Additional Reaction Steps for Hydroxyiodination of Anisole

step	reaction	rate law
4, 4R	$H^+ + HOI + AN \rightleftharpoons H_2OANI^+$	$-d[AN]/dt = k_4[H^+][HOI][AN] - k_{4R}[H_2OANI^+]$
6	$H_2OANI^+ \rightarrow ANI + H^+ + H_2O$	$-d[H_2OANI^+]/dt = k_6[H_2OANI^+]$
7	$H_2OANI^+ + IO_3^- + H^+ \rightarrow ANI + IO_3^- + H^+ + H_2O$	$-d[H_2OANI^+]/dt = k_7[H_2OANI^+][IO_3^-][H^+]$

TABLE 13: Average Rate Constants for the Reaction of I(I) withAnisole

step	value	comments
4	$k_4 = (5.22 \pm 0.36) \times 10^4\ M^{-2}\ s^{-1}$	least-squares fit
4R	$k_{4R} = 0.10\ s^{-1}$	arbitrary
6	$k_6 = 0.0195\ M^{-2}\ s^{-1}$	to fit $[IO_3^-]$ data
7	$k_7 = 10.0\ s^{-1}$	to fit $[IO_3^-]$ data

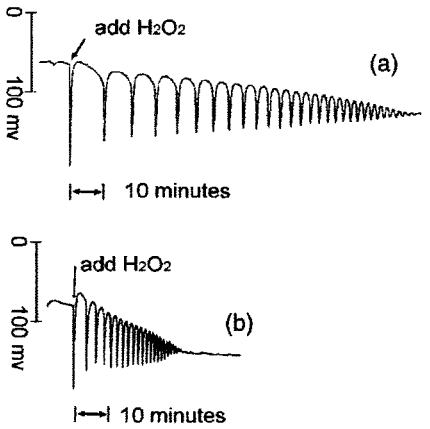

Figure 3. Potential (iodide-selective electrode vs Ag/AgCl) vs time for a crotonic acid oscillator. (a) $[HClO_4] = 0.106$ M, $[KIO_3] = 0.0100$ M, $[MnSO_4] = 0.0100$ M, $[CA] = 0.0150$ M, and $[H_2O_2] = 0.50$ M. (b) $[HClO_4] = 0.125$ M, $[KIO_3] = 0.0100$ M, $[MnSO_4] = 0.0100$ M, $[CA] = 0.040$ M, and $[H_2O_2] = 0.67$ M.

inversely dependent on [CA] and was sensitive to $[Mn^{2+}]$, with which the period length versus concentration goes through a maximum.

Crotonic acid was usually added from a stock solution. The order of reagents was usually perchloric acid, potassium iodate, manganese sulfate, crotonic acid, and hydrogen peroxide. The solution was protected from direct light.

Near the limit of a concentration range, only a few oscillations occurred, and they were damped, so we investigated the effect of added iodo product on the oscillations. We prepared iodohydrin in situ with CA, acid, KIO_3, and KI and waited until the I_2 color disappeared. There was very little effect when the initial [iodohydrin] was 0.0010 M.

Because the iodohydrin can be isolated and prepared separately, runs were made with the initial [iodohydrin] as high as 0.010 and 0.028 M. The amplitude and period of oscillations were decreased, but oscillations were still similar to those in solutions without iodohydrin.

We also investigated the effect of iodohydrin on I_2 production without CA present. In this case, there is a clear inhibiting effect of added iodohydrin. See Figure 4.

We also prepared the iodohydrin by adding I(III)[11] in H_2SO_4 to CA and waited until the disproportionation of I(III) to HOI and IO_3^- was nearly complete. Then $MnSO_4$ and H_2O_2 were added to start oscillations. At $[I(III)]_0 \gtrsim 1.6 \times 10^{-5}$ M, oscillations were completely prevented! Because the maximum [iodohydrin] in this experiment was only $\sim 1 \times 10^{-5}$ M and this concentration has little effect on the oscillator, there must be some unknown product that is a very effective inhibitor of oscillations.

4.3. Acrylic Acid Oscillators. The limiting ranges of oscillations with AC oscillators were not determined explicitly. Oscillations were found for $[H_2O_2]$ from approximately 0.67 to 1.0 M, for $[IO_3^-]$ from 0.0067 to 0.02 M, for $[Mn^{2+}]$ from 0.002 to 0.02 M, for [AC] from <0.033 to >0.155 M, and for $[HClO_4]$ from 0.1 to 0.138 M. See Figure 1S and Table 2S. The number

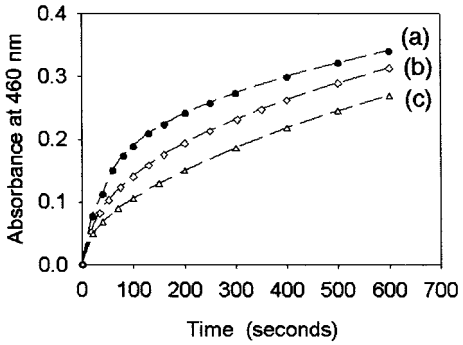

Figure 4. Absorbance at 460 nm vs time for nonoscillating, I_2-producing solutions including the effect of added iodohydrin. $[HClO_4] = 0.100$ M, $[KIO_3] = 0.0100$ M, $[MnSO_4] = 0.0020$ M, $[H_2O_2] = 1.0$ M. (a) [CAHOI] = 0. (b) [CAHOI] = 0.0231 M; (c) [CAHOI] = 0.0471 M.

of oscillations diminishes and the amplitude decreases as the limit of each concentration range is approached.

The initial excursion to low $[I^-]$ on adding H_2O_2 was usually much less than when CA was used. This was followed by an increase in $[I^-]$ and an induction period during which $[I^-]$ was significantly lower than when CA was used. The induction period increased with increasing [AC]. The length of each period decreased as the run proceeded.

Gas evolution was measured from one run using a gas buret. The rate of evolution was very low when $[I^-]$ was high, and a rapid increase in O_2 evolution occurred just after each excursion to low $[I^-]$, whereas $[I^-]$ was rapidly increasing. This behavior is similar to that of other BR oscillators.

Acrylic acid was usually added from a stock solution or as a pure liquid. The order of reagents was usually perchloric acid, potassium iodate, manganese sulfate, acrylic acid, and hydrogen peroxide. The solution was protected from direct light.

Several runs were made with iodohydrin generated in situ from iodate and I_2. At [iodohydrin] = 0.0012 M, the total length of the oscillations was less than half that of a mixture without initial iodohydrin. When iodohydrin was generated from I(III), however, a concentration of $\sim 6 \times 10^{-5}$ M was sufficient to prevent oscillations, which is very similar to the situation with crotonic acid.

Nonoscillatory mixtures with low ($\sim$0.1 M) H_2O_2 have an induction period that is longer with higher [AC]. After the induction period, absorbance in the UV increases dramatically (presumably from iodohydrin), although very little I_2 is formed. Other nonoscillatory conditions (low [AC]) act like clock reactions. There is a colorless induction period and then a sudden appearance of I_2.

4.4. *p*-Nitrophenol Oscillators. All the runs using *p*-nitrophenol (pNP) were highly damped. We never saw more than four oscillations, and frequently there was just one transition. See Figure 2S and Table 3S. For reasons that we were not able to determine completely, the reproducibility was troublesome, and period lengths were different even when conditions were apparently identical. Something on the order of 10% of the attempts to run oscillators failed. We investigated the stirring speed, order of addition of reagents, and delay between reagent addition. No changes in those parameters within reasonable limits seemed to have major effects. Light was excluded from the oscillating mixtures to avoid photoeffects. We did find that stock solutions of pNP that were more than a few days old seemed to act differently. We therefore weighed solid pNP as the first component and made sure that it had sufficient time to dissolve (a few minutes) before adding the

TABLE 14: Summary of Oscillating Mixtures under Similar Conditions[a]

substrate	oscillation range [substrate] (M)	midrange (M)	relative midrange [CA]/[substrate]	relative calculated (d[substrate]/d*T*)/d[CA]/d*t*
MeMA	0.0030−0.050	0.027	0.7	30−60
CA	0.011−0.030	0.020	1	1
AC	0.052−0.059	0.056	0.36	0.75
AN	0.0040−0.0096	0.0069	2.9	0.94
pNP	0.0120−0.0245	0.018	1.1	0.73

[a] Common concentrations were [$HClO_4$], 0.125 M; [KIO_3], 0.0067 M; [$MnSO_4$], 0.0033 M; and [H_2O_2], 1.0 M

other components. With most of these runs, the order of addition was pNP, water, acid, $MnSO_4$ solution, H_2O_2, and KIO_3.

All the components have minimum and maximum concentrations outside of which oscillations do not occur. Oscillations occur in a rather narrow region of concentrations of [KIO_3] or [H_2O_2], for which changes of 20% were sufficient to move outside the oscillatory range. The other components could be varied by up to 50%.

Addition of the last solution component caused a sharp change to very low [I^-], (see Figure 2S) followed by a rapid rise, a slow approach to a maximum, and a slow decrease. Finally, there was a sharp transition to low [I^-], which was similar to the very first low point. The cycle then repeated. The length of the first period was not very sensitive to concentration changes. Most periods were between 15 and 20 min. Likewise, the time from the first to the second transition was rather similar in all runs, mostly falling between 6 and 15 min. Each oscillation was shorter than the previous one in the same run and of smaller amplitude. Oscillations tended to end near the middle of the [I^-] range after a very weak transition.

Because the oscillations were so highly damped, we investigated the effect of the iodo product, in this case 2-iodo-4-nitrophenol (INP). We prepared INP in situ by adding either I_2 solution or KI solution to acidic iodate solution (with no H_2O_2 present). HOI from the hydrolysis of I_2 reacted with pNP to give INP. After a suitable delay (I_2 color disappearance), H_2O_2 was added. At $[INP]_0 = 0.001$ M, no oscillations were seen. At $[INP]_0 = 0.00025$ M, oscillations were seen, but the overall length was shortened by about 40%.

The rate of iodination of the substrate is governed by $d[INP]/dt = kN[HOI][INP]$. The formation of $\sim 5 \times 10^{-4}$ M INP in about 40 min (the time for oscillations to be completely damped) would require a [HOI] of about 5×10^{-8} M, a value that is consistent with estimated [HOI] in these solutions. We conclude that most of the damping is a result of INP formation and that the iodo product is a more effective radical trap than the original phenolic substrate.

The iodo product was also formed by adding I(III) in concentrated H_2SO_4 to the pNP solution. [$HClO_4$] was decreased to compensate for added H_2SO_4. I(III) hydrolyzes to IO_3^- and HOI. Assuming that there is no direct reaction with substrate and HIO_2, we predict that half of the initial iodine in I(III) should end as iodo product. An amount of I(III) equal to 6×10^{-4} M (giving 3×10^{-4} M [INP]) shortened the duration of the oscillations to about $^1/_4$ its value in the absence of I(III), roughly equivalent to the results of the experiment above where INP was added initially.

4.5. Anisole Oscillators. The vapor pressure of anisole in solution is sufficiently high that precautions must be taken to avoid losses during a run or from stock solutions. Our reactor vessel was tight enough to minimize this source of error, but some losses were inevitable during the mixing process. We used stock solutions to add anisole to the mixture and kept track of the stock solution concentration by absorbance. See Figure 3S and Table 4S.

The range of oscillations with AN oscillators has upper and lower concentration limits in all the components. They are somewhat interdependent, and roughly for [H_2O_2] from 0.86 to 2.0 M, for [IO_3^-] from 0.003 to 0.012 M, for [Mn^{2+}] from 0.0025 to 0.016 M, for [AN] from 0.004 to >0.0096 M, and for [$HClO_4$] from ~0.11 to >0.30 M, oscillations were found. The upper limit for [AN] was not reached because of limited solubility, and the upper limit for [$HClO_4$] appeared to be slightly above 0.30 M. The number of oscillations diminishes, and the amplitude decreases as the limit of each concentration range is approached.

Usually, the first period was longer (from 20 to 80%) than the subsequent periods. For oscillations near the middle of the range, the periods were relatively constant for more than 2 h. For the range of [AN] studied, the period increased with increasing [AN]. This trend is opposite to the effect of malonic acid and other enol-based substrates.

4.6. Comparison of Oscillators. We searched for a concentration condition where a methylmalonic oscillator could be compared with the substrates above, where only the substrate concentration was different. At $[HClO_4] = 0.125$ M, $[KIO_3] = 0.0067$ M, $[MnSO_4] = 0.0033$ M, and $[H_2O_2] = 1.0$ M, methylmalonic acid and all substrates named above produce oscillating systems for a range of substrate concentrations, although the pNP oscillator is highly damped. See Tables 5S and 14.

The fourth column in Table 14 was calculated relative to [CA] from the midrange values shown in column 3. The last column was calculated from the rate laws found for I_2 and substrate at $[H^+] = 0.125$ M and $[IO_3^-] = 0.0067$ M. (See section 3). Although the concentration ratios of the new substrates differ substantially (column 4), the relative substrate consumption rates (column 5) are similar, except for MeMA. There is a wide discrepancy between the reaction rate of MeMA and all the others, depending on the I_2 concentration. In general, both I_2 consumption rates and I_2 production rates are much slower in oscillators with the new substrates compared to that for MeMA.

5. Theory

Although the mechanism of the BR reaction is complex and not yet fully unraveled, R. M. Noyes and S. D. Furrow[12] and P. DeKepper and I. R. Epstein[13] proposed an 11-step kinetic skeleton model that accounts for the oscillatory behavior and the shape of oscillations for malonic acid oscillators. Some modifications have been proposed.[14,15] Work by Edelson[16] and Sörensen's group[17] has shown that the models reproduce the dynamics fairly well, although magnitudes and oscillation periods are not predicted well over the ranges of concentration of the initial reactants. Vukojevic et al.[18] claim that the further modifications and comparisons they have made reproduce behavior over a wider variety of conditions. Scaling to different concentrations is still a problem. More troubling is the fact that subsystems of the oscillating system (such as the acid, H_2O_2, IO_3^-, and Mn^{2+} subsystem that produces diiodine) are poorly represented by all variants of the skeleton mechanism.

As stated in the Introduction, the new substrates are iodinated by I(I), and there is indirect formation of iodide from I_2 hydrolysis. Although the stoichiometry is the same as with malonic acid, the dynamics are different. Substitution of iodination steps with the rate laws above does not lead to oscillatory behavior in a simulation using the models previously mentioned. Some other reaction is required with these substrates to get oscillations within the skeleton mechanism presented above, or changes are needed in the skeleton mechanism.

5.1. Changes to Skeleton Mechanism. The skeleton mechanism described above[12] has served well as a first approximation that reproduces some of the oscillatory features of the BR system. There are, however, some clear deficiencies, some of which we address further below. Those steps that have been retained from the original set are marked with an asterisk (*). The original designations are given on the left. We have made several modifications. With these modifications, oscillations are obtained with either methylmalonic acid or new substrates as the iodine sink.

Oxyiodine Reactions:

$$\text{I1*} \quad HOI + I^- + H^+ \leftrightarrow I_2 + H_2O \qquad (1,1R)$$

$$\text{I2*} \quad I^- + HIO_2 + H^+ \rightarrow 2HOI \qquad (2)$$

$$\text{I3*} \quad I^- + IO_3^- + 2H^+ \rightarrow HOI + HIO_2 \qquad (3)$$

$$\text{I5R*} \quad 2IO_2\bullet + H_2O \rightarrow HIO_2 + IO_3^- + H^+ \qquad (10)$$

The equilibrium constant for the overall hydrolysis of diiodine is well established, but there is no agreement on the rate constants for the forward and reverse steps, especially in acidic solutions. It is evident that there is more than one route for hydrolysis. Lengyel et al.[19] included a second step involving H_2IO^+ for which the rate of hydrolysis of diiodine is much higher than the rate we have used. We have opted to keep the hydrolysis rate at a lower value and to keep the model simple by omitting several known fast proton equilibria and the associated extra protonated species, assuming that they are in fast equilibrium.

Step 2 has been assumed to be very fast, but the value has never been measured directly, and the acid dependence has not been established. The Dushman reaction has complexities beyond those represented by step 3,[8,20] but the oscillation dynamics are not greatly affected by modest changes in k_3. Step 10 has not been measured; it has been considered to be fast. We have omitted the reverse of step 10 as a source of radicals. We have also omitted disproportionation of HIO_2, used by others,[12,13,15,18] believing the rate is much too slow[14].

Reactions Involving the Catalyst. In the original skeleton mechanism, all radicals are formed by a reaction that is the reverse of step 10 above. The radical $IO_2\bullet$ is then reduced by the metal catalyst.

$$\text{I5*} \quad IO_3^- + HIO_2 + H^+ \leftrightarrow 2IO_2C + H_2O$$

$$\text{M1*} \quad IO_2\bullet + Mn^{2+} + H_2O \rightarrow HIO_2 + Mn(OH)^{2+}$$

$Mn(OH)^{2+}$ was written as the dominant Mn(III) species at the usual pH used in the BR reactant mixtures. The combination of these two steps results in autocatalytic production of HIO_2. However, in a subsystem containing $IO_3^- + HIO_2 + H^+$ (where the HIO_2 disproportionates to IO_3^- and I_2), the additional presence of Mn^{2+} has little or no effect. Only when H_2O_2 and Mn^{2+} are present with oxyiodine species do we see a net reduction of oxyiodine species. We propose process 11 (not an elementary mechanistic step) to produce radicals.

$$HIO_2 + 2H_2O_2 + Mn^{2+} \rightarrow 2HOO\bullet + HOI + Mn^{2+} + H_2O \qquad (11)$$

This process preserves the autocatalytic production of HIO_2 when combined with steps 12 and 13 below. The process also actively produces HOI. Inclusion of this feature was key to getting oscillations with the new substrates. Other reductions of HIO_2 are too slow when $[I^-]$ is low to allow oscillations to develop.

We add the next group of reactions.

Reactions Involving the Reduction of Oxyiodine Species:

$$H^+ + IO_3^- + HOO\bullet \rightarrow IO_2\bullet + H_2O + O_2 \qquad (12)$$

$$IO_2\bullet + H_2O_2 \rightarrow HIO_2 + HOO\bullet \qquad (13)$$

$$\text{D1*} \quad HOI + H_2O_2 \rightarrow I^- + O_2 + H^+ + H_2O \qquad (14)$$

If previous step I5 is eliminated, some reduction process is necessary to bring iodine(V) into a lower state. We have added step 12 for that purpose. (The Dushman reaction, step 3, is too slow, as is the direct reduction of iodine(V) to iodine(III) by H_2O_2.) Step 12 was also used by Vukojevic et al.[18] in their model. The rate constant has not been measured. Cervellati et al.[21] have shown that several phenolic compounds and naturally occurring antioxidants have the ability to suppress oscillations in BR mixtures. They have ascribed that phenomenon to the scavenging of $HOO\bullet$ radicals by antioxidants, thereby competing with step 12. The rate for step 12 must be high enough to compete with disproportionation of $HOO\bullet$ radicals, step 17 below.

Step 13 was included to produce HIO_2. When coupled with steps 11, 12, and 13 under conditions of low $[I^-]$, HIO_2 is produced autocatalytically, preserving the overall oscillation dynamics of previous models. The rates of steps 11 and 10 must be comparable during diiodine production.

The rate constant for step 14 was measured by Liebhafsky.[22] Furrow found a lower value[14] and in fact, under conditions of very low $[I^-]$, found that H_2O_2 oxidized HOI. The higher value for k_{D1} used by Sörensen's group[18] is much larger than either of those values.

The specifics of manganese ion involvement are unknown and are incorporated in step 11 above. The previously included reduction of Mn(III) by H_2O_2

$$\text{M2*} \quad Mn(OH)^{2+} + H_2O_2 \rightarrow Mn^{2+} + H_2O + HOO\bullet$$

may be a substep of step 11. It is fast enough so that it is not rate-determining, and it has been omitted from this scheme.

Organic Substrate—Iodine Reactions:

$$\text{R1*} \quad CH_2(COOH)_2\,(\text{diacid}) \rightleftarrows (HOOC)CH{=}C(OH)_2\,(\text{enol}) \qquad (15)$$

$$\text{R2*} \quad (HOOC)CH{=}C(OH)_2\,(\text{enol}) + I_2 \rightarrow IHC(COOH)_2 + I^- + H^+ \qquad (16)$$

$$H^+ + HOI + \text{substrate} \rightarrow H^+ + \text{iodohydrin or iodosubstrate} + H_2O \qquad (4)$$

As can be seen in this modified skeleton mechanism, the organic substrate acts only as a sink for iodine and as a source

TABLE 15: Rate Laws Used for Simulation

step	rate law	reference
1	$3.67 \times 10^9[HOI][I^-]$	from K[19] and step 1R (see text)
1R	$0.00198[I_2]/[H^+]$	19
2	$5.0 \times 10^9\ M^{-1}[I^-][HIO_2]$	arbitrary, fast
3	$1430\ M^{-1}[H^+]^2[I^-][IO_3^-]$	20
10	$5 \times 10^9[IO_2C]^2$	this work, estimated
11	$31\,000[H_2O_2][Mn^{2+}][HIO_2]$	this work, estimated
12	$1.3 \times 10^4[H^+][IO_3^-][HOO\bullet]$	this work, estimated
13	$20[H_2O_2][IO_2\bullet]$	this work, estimated
14	$5[HOI][H_2O_2]$	14
15	1.6×10^{-4}[MeMA]	23
15R	1[enol]	23
16	$1 \times 10^5[enol][I_2]$	23
17	$7.5 \times 10^5[HOO\bullet]^2$	24

of iodide ion for malonyl derivatives. For other substrates, there is the formation of iodide from iodine hydrolysis.

The BR oscillator is, in fact, considered to be a halate-driven oscillator controlled by halide ions in the sense that oscillations of all intermediates arise because of the periodic consumption and formation of iodide ions.

Reactions Involving Oxygen Species:

$$O2^* \qquad 2HOO\bullet \rightarrow H_2O_2 + O_2 \qquad (17)$$

Steps 12, 14, and 17 involve reactions that lead to the formation of O_2. The formation of O_2 gas bubbles can be observed during the course of the reaction.

Rate laws used for the simulation are given in Table 15.

5.2. Comparison with Experiment. Simulations have been run using the steps above at the following reference concentrations: $[HClO_4] = 0.125$ M, $[KIO_3] = 0.0067$ M, $[MnSO_4] = 0.0033$ M, and $[H_2O_2] = 1.0$ M. There is a problem in the choice of parameters for the model because even with enolic substrates such as methylmalonic acid it has not been possible to reproduce both the maximum $[I_2]$ and the period in any one run. If the maximum $[I_2]$ is correct, then the minimum $[I_2]$ is much too low in the simulations. The periods are much too long because of the time required for $[I_2]$ to decrease to the minimum, where it switches.

Some sample comparisons between experiment and simulation are shown in Figures 5 and 6 for a methylmalonic acid oscillator. Although the log[I⁻] simulation compares reasonably well with experiment, the simulated $[I_2]$ decreases much too far. The measured absorbance at 460 nm for the same conditions varied from approximately 0.09 (maximum) to about 0.055 (minimum). A problem with matching the experimental period arises because of this difficulty. (The same problem applied to the previous skeleton mechanism).

A summary of comparisons of simulations with experiment using the new substrates is shown in Table 16.

The calculated ranges of substrate concentration where oscillations generally occur overlap the experimental ranges,

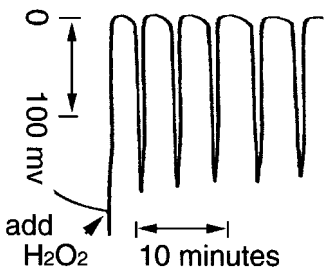

Figure 5. Simulations of log[I⁻] vs time and absorbance vs time for a methylmalonic acid oscillator. $[HClO_4] = 0.125$ M, $[KIO_3] = 0.0067$ M, $[MnSO_4] = 0.0033$ M, [MeMA] = 0.0106 M, $[H_2O_2] = 1.00$ M.

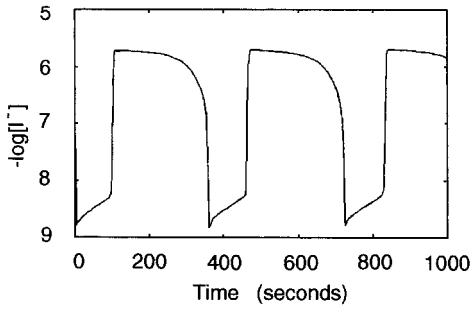

Figure 6. Experimental absorbance at 460 nm vs time for a crotonic acid oscillator. $[HClO_4] = 0.125$ M, $[KIO_3] = 0.0067$ M, $[MnSO_4] = 0.0033$ M, [CA] = 0.017 M, $[H_2O_2] = 1.00$ M.

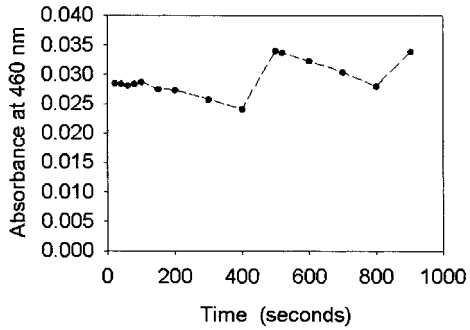

Figure 7. Simulations of absorbance at 460 nm vs time and log[I⁻] vs time for a crotonic acid oscillator. $[HClO_4] = 0.125$ M, $[KIO_3] = 0.0067$ M, $[MnSO_4] = 0.0033$ M, [CA] = 0.017 M, $[H_2O_2] = 1.00$ M.

but the calculated ranges are wider and require higher substrate concentrations than those that are found experimentally. The oscillation periods do not agree well with any of the substrates. The dependence on concentration with AN is in the wrong direction. The I_2 concentration with the new substrates in the simulations varies less from the maximum to the minimum than it does with methylmalonic acid. This result is similar to the experimental observations, but the magnitude is higher in the simulation than in the experimental results.

Experimental and simulation absorbances and log[I⁻] values are shown for a CA oscillator in Figures 7 and 8. Here, the relative shapes of both absorbance and log[I⁻] are in better

TABLE 16: Comparison of Experiment with Simulation[a]

substrate	oscillation range experimental [substrate] (M)	oscillation range calculated [substrate] (M)	average of first and second period experimental (s)	period calculated (s)
MeMA	0.0030−0.050[b]	0.003−0.050[b]	1230−55	2200−25
CA	0.011−0.030	0.015−0.025	160−130	6000−2400
AC	0.052−0.059	0.063−0.10	1700−1500	2400−950
AN	0.0040−0.0096	0.0074−0.012	600−1000	4300−1400
pNP	0.0120−0.0245	0.023−0.037	900−700	3500−1000

[a] Common concentrations were $[HClO_4]$, 0.125 M; $[KIO_3]$, 0.0067 M; $[MnSO_4]$, 0.0033 M; and $[H_2O_2]$, 1.0 M [b] Highest concentration studied. The maximum concentration with oscillations is higher.

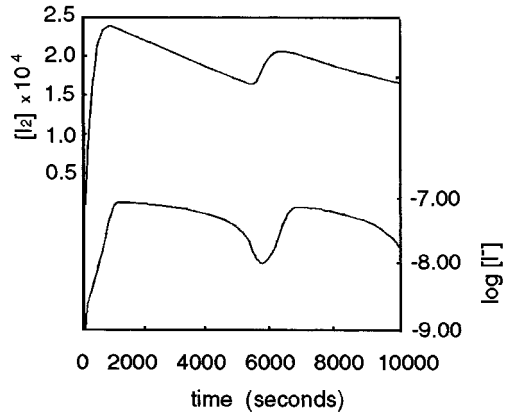

Figure 8. log[I^-] vs time for a methylmalonic acid oscillator using an iodide-selective electrode vs Ag/AgCl. [$HClO_4$] = 0.125 M, [KIO_3] = 0.0067 M, [$MnSO_4$] = 0.0033 M, [MeMA] = 0.0106 M, [H_2O_2] = 1.00 M.

agreement, but the magnitude of the simulated absorbance is too large. As stated above, the calculated period is much too long.

The iodo products and possible oxidation products of each of the new substrates undergo additional inhibitory reactions with radicals, HOI, or HIO_2. We have not attempted to simulate those complications.

5.3. Conclusions. BR oscillators with the new substrates undergo oscillations within certain concentration limits. Neither the original skeleton mechanism nor more recent modifications are able to simulate this behavior. Within that mechanism, the transition from low [I_2] and low [I^-] to high concentrations of both species depends on the production of iodide ion from the reduction of HOI by H_2O_2 and the formation of I^- as the methylenic substrate forms an enol to react with I_2. The new substrates effectively compete for HOI and prevent either I_2 or I^- from accumulating. An active route other than I^- is required to produce HOI from HIO_2. Such a process has been included, although mechanistic details have been bypassed by using an overall process. With the process included, simulation of oscillations is possible using iodination rate constants measured separately, although the agreement is qualitative, at best. A suggestion has also been made that the main route for the reduction of IO_3^- is by HOO• radicals instead of by reaction with HIO_2.

There are still significant unresolved issues with the BR mechanism. When no manganese is present in iodate−I_2−hydrogen peroxide mixtures, there is definite oxidation of both HOI and HIO_2. These steps have been omitted from the BR mechanism. There are interactions with organic components that are not understood. Few of the rate laws for oxyiodine−hydrogen peroxide reactions have been confirmed. Ultimately, oxidation of I_2 to iodate, reduction of iodate to I_2, and the steps in the BR oscillator should all include common steps.

Acknowledgment. This work was supported financially in part by funds for selected research topics (Università di Bologna).

Supporting Information Available: Tables 1S−5S contain concentration conditions for oscillations for oscillators containing CA, AC, pNP, and AN, and a comparison of oscillators with different substrates under similar conditions, respectively. Figures 1S−3S contain data for [I^-] versus time for oscillators containing AC, pNP, and AN, respectively. This material is available free of charge via the Internet at http://pubs.acs.org.

References and Notes

(1) Furrow, S. D.; Noyes, R. M. *J. Am. Chem. Soc.* **1982**, *104*, 38.
(2) Briggs, T. S.; Rauscher, W. C. *J. Chem. Educ.* **1973**, *50*, 496.
(3) Furrow, S. D. *J. Phys. Chem.* **1995**, *99*, 11131.
(4) Furrow, S. D. *J. Phys. Chem.* **1982**, *86*, 3089.
(5) Furrow, S. D. *Int. J. Chem. Kinet.* **1982**, *14*, 927.
(6) Furrow, S. D.; Noyes, R. M. *J. Am. Chem. Soc.* **1982**, *104*, 42.
(7) Some of this work has been presented by Amadori, G. *Nuovi Substrati e Catalizzatori per la Reazione Oscillante di Briggs−Rauscher ed Effeti Inibitori di Alcuni Additivi* (in Italian, abstract in English), Laurea Thesis, Faculty of Pharmacy, University of Bologna, Bologna, Italy, 1998.
(8) Agreda, J. A.; Field, R. J.; Lyons, N. J. *J. Phys. Chem.* **2000**, *104*, 5269.
(9) Mendes, P. *GEPASI*: A Software Package for Modeling the Dynamics, Steady States, and Control of Biochemical and Other Systems. *Comput. Appl. Biosci.* **1993**, *9*, 563−571. Mendes, P. *Trends Biochem. Sci.* **1997**, *22*, 361−363. Mendes, P.; Kell, D. B. *Bioinformatics* **1998**, *14*, 869−883.
(10) The HPLC studies were done with the assistance of Professor Anna Maria Di Pietra, Dipartimento di Scienze Farmaceutiche, University of Bologna.
(11) Noszticzius, Z.; Noszticzius, E.; Schelly, Z. A. *J. Phys. Chem.* **1983**, *87*, 510.
(12) Noyes, R. M.; Furrow, S. D. *J. Am. Chem. Soc.* **1982**, *104*, 45.
(13) DeKepper, P.; Epstein, I. R. *J. Am. Chem. Soc.* **1982**, *104*, 46.
(14) Furrow, S. D. *J. Phys. Chem.* **1987**, *91*, 2129.
(15) Turányi, T. *React. Kinet. Catal. Lett.* **1991**, *45*, 235.
(16) Edelson, D. *J. Phys. Chem.* **1983**, *87*, 1204.
(17) Vukojevic, V., Sörensen, P. G.; Hynne, F. J. *J. Phys. Chem.* **1993**, *97*, 4091.
(18) Vukojevic, V.; Sörensen, P. G.; Hynne, F. J. *J. Phys. Chem.* **1996**, *100*, 17175.
(19) Lengyel, I.; Li, J.; Kustin, K.; Epstein, I. R. *J. Am. Chem. Soc.* **1996**, *118*, 3708.
(20) Furuichi, R.; Liebhafsky, H. A. *Bull. Chem. Soc. Jpn.* **1975**, *48*, 745.
(21) Cervellati, R.; Crespi-Perellino, N.; Furrow, S. D.; Minghetti, A. *Helv. Chim. Acta* **2000**, *83*, 3179−3190. Cervellati, R.; Höner, K.; Furrow, S. D.; Neddens, C.; Costa, S. *Helv. Chim. Acta* **2001**, *84*, 3533.
(22) Liebhafsky, H. A. *J. Am. Chem. Soc.* **1932**, *54*, 3504.
(23) Furrow, S. D. *J. Phys. Chem.* **1981**, *85*, 2026.
(24) Behar, D.; Czapski, G.; Dorfman, L. M.; Schwartz, H. A. *J. Phys. Chem.* **1970**, *74*, 3209.